

Sensitivity of young water fractions to hydro-climatic forcing and landscape properties across 22 Swiss catchments

5 **Jana von Freyberg et al.**

Correspondence to: Jana von Freyberg (jana.vonfreyberg@usys.ethz.ch)

- Table S1 with additional data about elevation ranges, the phases of the seasonal precipitation regimes, as well as hydrologic soil properties and hydrogeological characteristics of the
10 individual sites
- Detailed description of an alternative interpolation method for precipitation isotopes (method 2)
- *R* script for performing iteratively reweighted least squares (IRLS) regression with optional point weights, including a demo data set (temporary filename “*IRLS_hess-2017-720.R*”)

15

20

Table S1: Elevation ranges, as well as hydrologic soil properties and hydrogeological characteristics of the 22 Swiss study catchments.

| Catchment name | Minimum elevation (m a.s.l.) | Maximum elevation (m a.s.l.) | Phase of seasonality of monthly precipitation φ_{precip} (months) | Fraction of shallow soils (%) | Fraction of low - medium water storage capacity soils (%) | Fraction of high - very high permeability soils (%) | Fraction of aquifers with low productivity (%) | Fraction of aquifers with intermediate productivity (%) | Fraction of aquifers with high productivity (%) |
|--------------------|------------------------------|------------------------------|--|-------------------------------|---|---|--|---|---|
| Aabach | 519 | 1092 | 3.8 | 0 | 0 | 23 | 87 | 0 | 13 |
| Aach | 408 | 560 | 3.9 | 0 | 0 | 0 | 86 | 0 | 14 |
| Allenbach | 1293 | 2742 | 3.2 | 78 | 57 | 30 | 89 | 11 | 0 |
| Alp | 845 | 1894 | 3.2 | 68 | 48 | 1 | 81 | 6 | 12 |
| Biber | 827 | 1495 | 3.3 | 30 | 30 | 0 | 94 | 0 | 6 |
| Dischmabach | 1663 | 3139 | 3.5 | 59 | 59 | 59 | 92 | 9 | 0 |
| Emme | 743 | 2216 | 3.3 | 78 | 49 | 21 | 88 | 11 | 0 |
| Ergolz | 305 | 1165 | 4.0 | 42 | 41 | 28 | 42 | 54 | 5 |
| Erlenbach | 1117 | 1650 | 3.2 | 100 | 4 | 0 | 82 | 18 | 0 |
| Guerbe | 556 | 2152 | 3.6 | 48 | 35 | 45 | 70 | 17 | 13 |
| Ilfis | 681 | 2087 | 3.3 | 32 | 28 | 42 | 92 | 1 | 7 |
| Langeten | 598 | 1100 | 3.4 | 0 | 0 | 37 | 77 | 13 | 10 |
| Lümpenenbach | 1092 | 1508 | 3.1 | 100 | 4 | 0 | 100 | 0 | 0 |
| Mentue | 447 | 926 | 4.7 | 0 | 0 | 76 | 99 | 0 | 0 |
| Murg | 467 | 1036 | 3.7 | 0 | 0 | 9 | 87 | 1 | 12 |
| Ova da Cluozza | 1519 | 3160 | 3.4 | 34 | 34 | 34 | 8 | 92 | 0 |
| Riale di Calneggia | 881 | 2908 | 3.3 | 39 | 44 | 44 | 96 | 4 | 0 |
| Rietholzbach | 671 | 938 | 3.7 | 0 | 0 | 0 | 100 | 0 | 0 |
| Schacchen | 487 | 3260 | 3.5 | 73 | 67 | 23 | 76 | 24 | 0 |
| Sense | 554 | 2184 | 3.6 | 39 | 24 | 47 | 85 | 10 | 5 |
| Sitter | 768 | 2500 | 3.2 | 71 | 61 | 36 | 48 | 52 | 0 |
| Vogelbach | 1038 | 1540 | 3.2 | 100 | 51 | 0 | 100 | 0 | 0 |

An alternative interpolation method for precipitation isotopes (method 2)

Precipitation $\delta^{18}\text{O}$ measurements from 19 long-term monitoring stations in Switzerland (13 stations from NAQUA-ISOT, the Swiss network for Observations of Isotopes in the Water Cycle) and Germany (6 stations from GNIP, the Global Network of Isotopes in Precipitation) were decomposed into sine functions and time series of residuals from the sine functions. The measurements were fitted to sine curves through least squares regression:

$$c(t) = A \sin(2\pi f t - \varphi) + k \quad (\text{S1})$$

In Eq. (S1), A is the amplitude (‰), φ is the phase of the seasonal cycle (rad, with 2π rad equalling 1 year), t is the time (decimal years), f is the frequency (1 year^{-1}) and k (‰) is a constant describing the vertical offset of the isotope signal. The mean RMSE for the sine fits across all measurement stations was 2.1 ‰ $\delta^{18}\text{O}$.

Each of the three parameters describing the best-fit sine functions (A , φ , and k) of the 19 long-term monitoring stations were interpolated for all of Switzerland using multiple linear regression models based on latitudes, longitudes, and elevations:

$$A = 0.0002 \cdot \text{elevation} + 0.22 \cdot \text{longitude} - 0.88 \cdot \text{latitude} + 3.97 \quad (\text{S2})$$

$$\varphi = -3.47 \cdot 10^{-5} \cdot \text{elevation} + 0.007 \cdot \text{longitude} + 0.049 \cdot \text{latitude} - 1.82 \quad (\text{S3})$$

$$k = -0.0025 \cdot \text{elevation} - 0.38 \cdot \text{longitude} + 0.50 \cdot \text{latitude} - 10.4 \quad (\text{S4})$$

The explanatory variables in Eqs. (S2) - (S4) have been centered around their means, so that the intercepts describe the average latitudes, longitudes and elevations of the 19 stations, rather than an extrapolation to the arbitrary values latitude=0, longitude=0, and elevation=0.

The performance of the multiple-regression models that describe the spatial variations of the best-fit sine functions was quantified by RMSE, R^2 and the p -values of the individual coefficients (Table S2):

Table S2: RMSE, R^2 and the p -values of the individual coefficients of the multiple-regression models.

| | RMSE | R^2 | Elevation (p value) | Longitude (p value) | Latitude (p value) | Intercept (p value) |
|---------------------------------------|---------|-------|---------------------------|---------------------------|--------------------------|---------------------------|
| Amplitude A | 0.70‰ | 0.56 | 0.62 | 0.16 | 0.004 | $1.6 \cdot 10^{-13}$ |
| Phase of the seasonal cycle φ | 0.09rad | 0.29 | 0.51 | 0.72 | 0.15 | $5.8 \cdot 10^{-22}$ |
| Constant k | 0.66‰ | 0.87 | 0.00001 | 0.01 | 0.06 | $3.25 \cdot 10^{-20}$ |

It should be noted that the three station properties were not strongly correlated with one another (i.e., $R=0.23$ and $p=0.35$ for elevation versus longitude; $R=-0.42$ and $p=0.07$ for elevation versus latitude;

$R=0.30$ and $p=0.21$ longitude versus latitude). The linear regression models were used to model sine parameters (A , ϕ , and k) for every 200m pixel in the 22 Swiss study catchments.

In a second step, the time series of residuals from the sine functions were geostatistically interpolated for every month of the time period 2010-2015 and every 200m pixel in the 22 Swiss study catchments.

- 5 The spatial interpolation was carried out through ordinary kriging, applying an exponential variogram model. Monthly maps of residuals from the sine functions were then used to adjust the base sinusoidal pattern for each 200m pixel.

- To quantify the prediction error of this interpolation method, it was run iteratively to simulate the monthly precipitation isotopic composition for each of the 19 long-term monitoring stations. For each
10 of the 19 iterations, the precipitation isotope time series was predicted for one station by using only the remaining 18 stations for calibration (i.e., a leave-one-out process). This two-step approach resulted in a 1.3 ‰ $\delta^{18}\text{O}$ mean absolute deviation between observations and model outputs.

- For this interpolation method, monthly isotope values were volume-weighted for each pixel based on the monthly elevation-dependent precipitation volumes obtained from the PREVAH model (Viviroli et
15 al., 2009). Next, the monthly precipitation isotope values were aggregated across all 200m pixels in each catchment for a volume-weighted, catchment-averaged precipitation isotope time series. Snow accumulation and melt were not distinguished from liquid precipitation; that is to say, precipitation was treated as a direct input to the catchment at time of falling and snowpack storage was considered to be part of catchment storage (see Sect. 4.2 in main text).

- 20 The mass-weighted, catchment-averaged precipitation isotope time series were used for obtaining the parameter A_P (Eqs. (1), (3), and (5) in the main text). For the 22 study catchments, the approach presented above resulted in different A_P values compared to those obtained by the approach of Seeger and Weiler (2014); the method of Seeger and Weiler (2014) predicted higher A_P values for higher elevation sites (Fig. 3 in the main text). In applying the alternative method described here, we find that
25 elevation is a weak predictor of seasonal cycle amplitudes A (Table S2). In contrast to the Seeger and Weiler (2014) method, we find that A was primarily controlled by latitude and longitude, resulting in the largest A_P values for catchments in south-eastern Switzerland. However, spatial variations in $\delta^{18}\text{O}$ in precipitation are not simply a product of elevation (Seeger and Weiler, 2014) or of elevation, latitude, and longitude (alternative method), because both the Seeger and Weiler (2014) method and the
30 alternative method presented here used kriging to incorporate other possible isotope effects.

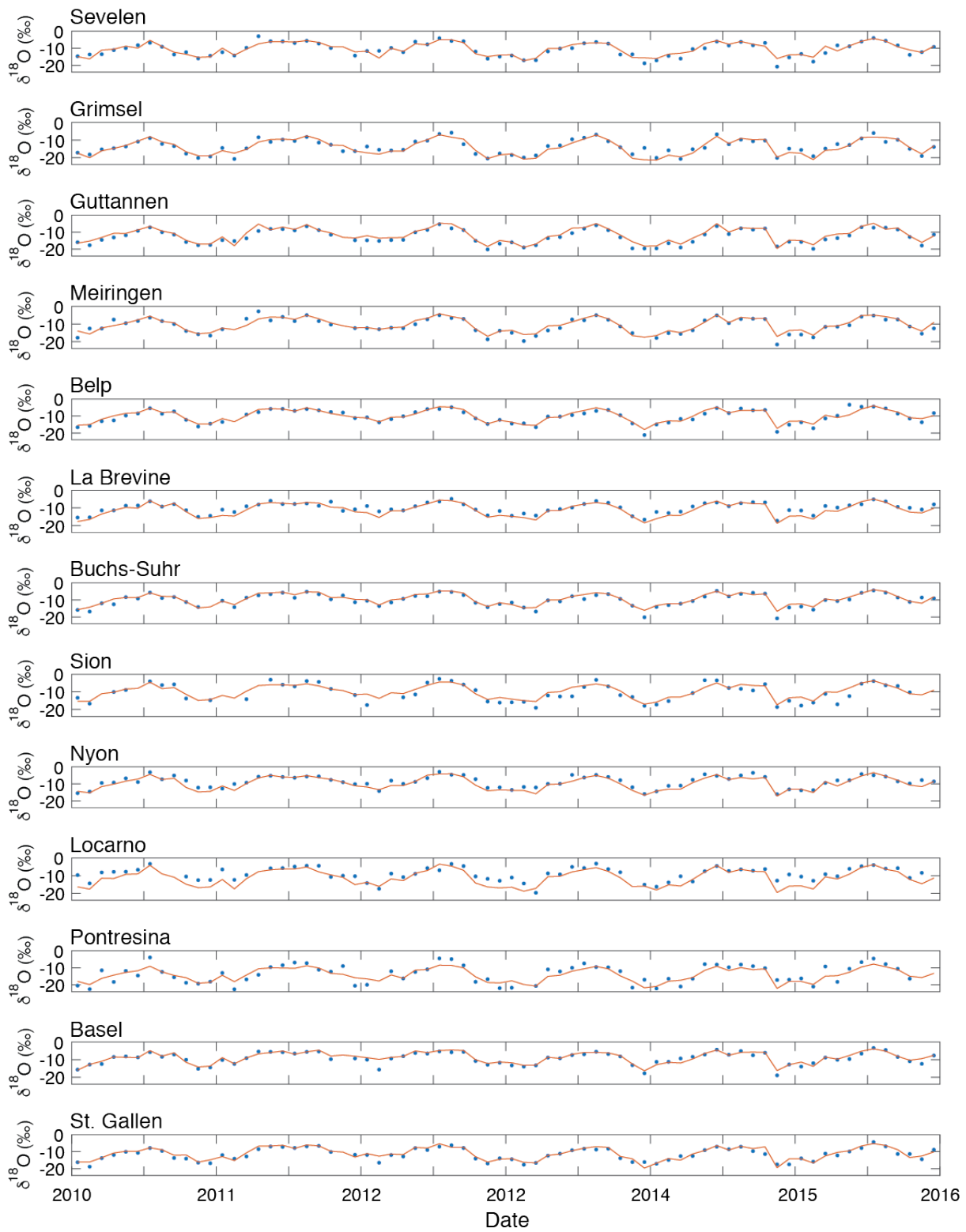


Figure S1: Modelled monthly isotope ($\delta^{18}\text{O}$) time series predicted for the 13 Swiss long-term monitoring stations. The precipitation isotope time series were predicted for one station at a time by using only the remaining 18 stations (the other 12 Swiss stations and 6 German stations) for calibration (i.e., a leave-one-out process). Dots indicate the monthly observations, while lines indicate the modelled time series.

Table S 3: Long-term monitoring stations with their latitudes, longitudes and elevations used for the interpolation method presented here.

| Long-term monitoring station | Latitude | Longitude | Elevation (m a.s.l.) |
|------------------------------|----------|-----------|-------------------------|
| Sevelen (CH) | 47.12 | 9.49 | 457 |
| Grimsel (CH) | 46.57 | 8.33 | 1950 |
| Guttannen (CH) | 46.66 | 8.29 | 1055 |
| Meiringen (CH) | 46.73 | 8.18 | 632 |
| Belp (CH) | 46.90 | 7.51 | 515 |
| La Brevine (CH) | 46.98 | 6.61 | 1042 |
| Buchs-Suhr (CH) | 47.37 | 8.08 | 397 |
| Sion (CH) | 46.22 | 7.34 | 482 |
| Nyon (CH) | 46.38 | 6.23 | 436 |
| Locarno (CH) | 46.17 | 8.79 | 379 |
| Pontresina (CH) | 46.49 | 9.90 | 1742 |
| Basel (CH) | 47.54 | 7.58 | 319 |
| St.Gallen (CH) | 47.43 | 9.42 | 805 |
| Konstanz (GER) | 47.68 | 9.19 | 443 |
| Weil am Rhein (GER) | 47.60 | 7.59 | 249 |
| Karlsruhe (GER) | 49.04 | 8.37 | 112 |
| Hohenpeissenberg (GER) | 47.80 | 11.01 | 977 |
| Stuttgart (GER) | 48.83 | 9.20 | 314 |
| Garmisch-Partenkirchen (GER) | 47.48 | 11.06 | 719 |

5 References

Seeger, S., and Weiler, M.: Reevaluation of transit time distributions, mean transit times and their relation to catchment topography, *Hydrol. Earth Syst. Sci.*, 18, 4751-4771, 2014.

Viviroli, D., Zappa, M., Gurtz, J., and Weingartner, R.: An introduction to the hydrological modelling system PREVAH and its pre- and post-processing-tools, *Environmental Modelling & Software*, 24, 1209-1222, 10.1016/j.envsoft.2009.04.001, 2009.

10